# A Disposal of the Space Debris with Special Spacecraft Debris Collector using Low Trust

Sergey A. Ishkov and Gregory A. Filippov

***Abstract*—the aim of this work is to study the possibility of the disposal of the space debris in the dense layers of the Earth's atmosphere. We use information about the fragments of the space debris location that stored in NORAD databases. There two types of the orbits of the space debris are explored: the high elliptical orbit and the circular orbits. The algorithm of the operation of the utilization of the fragments of the space debris in the dense layers of the Earth's atmosphere using the special spacecraft debris collector is composed. The spacecraft debris collector must be equipped with electro propulsion engines with low-thrust. The mathematical model of the plane motion of the spacecraft debris collector, in the form of the system of osculating elements, is composed. Problem of the descent of the fragments of the space debris reduced to the problem of the reducing of the height of the perigee of elliptical orbit. Obtained the locally - optimal control program of the orientation of the thrust vector. Using the L.S. Pontryagin's maximum principle, we solved the boundary value problem of the optimal control (decrease) of the perigee of the elliptical orbit. The results of the parametric study of the problem in the space of the initial orbits and the acceleration traction of the electro propulsion engines is shown. Numerical simulation of the space debris reduction from the low circular orbits is performed. Determined the number of revolutions passed a fragment of the space debris around the Earth during braking due to aerodynamic drag. Calculated the estimates of the gains of the characteristic velocity to perform the operation.**

***Index Terms*—disposal of the space debris, descent space debris, orientation of the vector of the jet thrust, optimum control on the orb, reducing the height of perigee, the trajectory in the atmosphere, characteristic velocity.**

## I. Introduction

THE problem of the disposal of the space debris (e.g. SD) is coming more popular with the expansion of human space activities. Fragments of the SD scattered in almost all heights of the circumterrestrial space, which poses a risk to an operational satellites and creates additional difficulties for launch of new satellites.

Identification of the potentially dangerous objects of the SD considered in [1, 2]. These articles are given characteristics of the orbits of the SD. More information about the orbits of the SD can be founded in the NORAD's catalog databases of space objects [3, 4].

Sergey A. Ishkov Ph.D of Technical Science at the Samara State Aerospace University named after academician S.P. Korolev (National Research University), department of spacecraft design.

Gregory A. Filippov (corresponding author) specialist, engineer of the Samara State Aerospace University named after academician S.P. Korolev (National Research University), e-mail: grigory_ssau@mail.ru

To solve the problem of the disposal of the SD offers an active and a passive method. A passive method involve the implementation of the preventive measures. It aimed a preventing of the creation of a new space debris in the process of the space activities: the forced reduction to the atmosphere of a spacecraft, whose life is end [5,6]. Nowadays passive measures of the disposal of the SD is not enough. In the orbits continue its existence the fragments of the SD left over from the previous starts. The results in the article [7] shown, that the population of the SD over time will grow up as the result of collisions and damage already retired uncontrol objects.

Active ways for solving of this problem include the transition of the fragments of the SD to the low orbits for the subsequent occurrences of the fragments of the SD to the dense layers of the Earth atmosphere. For the transition of the fragments of SD in the Earth's atmosphere will need the special vehicle – the Spacecraft Debris Collector (e.g. SDC). Most suitable for this purpose is a spacecraft equipped with the electric propulsion engine with low – trust. This type of spacecraft allows an active transport operations for a long time [8 – 10].

For fixing of the fragments of the SD on board of the SDC require special facilities and equipment. The articles [11 – 12, 33] proposes to use for this purpose a space tether systems. Explores in detail the movement of the system SD – SDC around the mass center.

There are projects that use a high-power pulsed laser system for braking space objects and placing them on a descent trajectory [13, 14]. We suggest to using a special manipulator «robotic arm» [15, 30], which rigidly fixes the fragment of the SD aboard the SDC. The problems of the control of some of the «robotic arms» discussed in article [34].

It is needed to note, that the large fragments of the SD are the most dangerous. This type of the fragments of the SD can not completely burn up in the Earth's atmosphere. It can cause the destruction for the earthly objects [16]. For these fragments of the SD we must provide descent to the predetermined disposal area. If SDC contains pulse brake motors, so operation is not a difficult technical problem. But electric propulsion engine with low – trust can not provide the traditional scheme of descent.

This article discusses the problem of the control of the SDC for disposal of the fragments of the SD to the predetermined disposal area. We have considered variants of descent of the fragments of the SD from the elliptical and circular orbits. We assume that the SDC approached with the fragment of the SD and fixed it. We pose the problem of the synthesis of the control program for the SDC for descent the fragment of the SD from elliptical orbit to the

(Advance online publication: 24 April 2015)

predetermined area of the Earth surface. We propose the following scheme of descent:

(i) The SDC with the fragment of the SD transferred to the orbit elliptical with an extremely small margin of the height of the perigee (about 200 km). The remaining orbital parameters (esp. argument of perigee and the longitude of the ascending node (see section III.E)) is chosen to ensure the descent of the fragment of SD to the predetermined area of the Earth surface.

(ii) At a predetermined orb, at moment of passing of perigee, the propulsion system of the SDC switched on with the predetermined orientation of the thrust vector(see sections II.B and II.C). In this case, the thrust vector is aimed at the maximum reduction of the height of perigee.

(iii) Operation of the engine at this program will continue until the SDC reaches the apocenter of the orbit (see section III.B). At this moment the fragment of the SD disconnect from the SDC, propulsion system switches to the control, which provide the maximum rate of increasing of the height of the perigee [31].

(iv) The fragment of the SD performs the passive flight and near pericentre of the orbit it enter to the dense layers of the atmosphere and descent in the predetermined area of the Earth surface (it is considered in the sections II.E, III.C, III.D and III.E).

(v) SDC during the remaining part of the orb should increase the height of the perigee to secure (about 200 km) and make an orbital transfer to the target orbit in accordance with its program.

As the fragment of the SD, we considered defective and/or does not operating spacecraft, wreckage of boosters and other man – made objects in Space.

## II. Mathematical Models

Let us study the feasibility of this scheme of the disposal of the SD from the elliptical orbit. We define the optimal control program of the thrust vector orientation.

### *A. The Planar Motion of SDC*

Planar motion of a spacecraft with electric propulsion engine with low – thrust can be described by the system of differential equations of the form:

$$
\begin{aligned}
\frac{dp}{dt} &= 2rw\sin\lambda\sqrt{\frac{p}{\mu}} \\
\frac{de}{dt} &= w\cos\lambda\sqrt{\frac{p}{\mu}}\sin\vartheta + \left[\cos\vartheta + (e+\cos\vartheta)\frac{r}{p}\right]w\sin\lambda\sqrt{\frac{p}{\mu}} \\
\frac{d\vartheta}{dt} &= \sqrt{\frac{p}{\mu}}\left[\frac{\mu}{r^2} + w\cos\lambda\frac{\cos\vartheta}{e} - w\sin\lambda\left(1+\frac{r}{p}\right)\frac{\sin\vartheta}{e}\right]^{-1}
\end{aligned}
\qquad (1)
$$

where $p$ – focal parameter of the orbit, $r$ – geocentric distance $r = p\cdot(1+e\cdot\cos\vartheta)$, $\vartheta$ – true anomaly, $\mu$ – Earth's gravitational parameter $398600{,}4\,km^3/s^2$, $\lambda$ – the angle between the thrust of the jet and the radius vector in the orbital plane (see fig. 1), $w$ – thrust acceleration.

The angle $\lambda$ is the single control parameter, due to the engine is not turn off and it engine is not regulated (see Fig. 1).

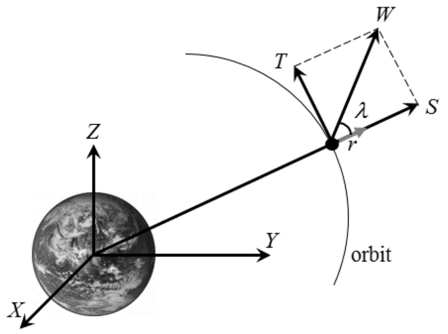


Fig. 1 The orientation of the angle $\lambda$

We assume that the acceleration is small, compared to Gravity, and $w/e \ll \mu/p^2$. On this basis, we will make the transition to the new independent variable – the eccentric anomaly $E$, using replacement:

$$
dE = \sqrt{\frac{\mu\cdot\left(1-e^2\right)^3}{p^3}}\cdot\left(1-e\cdot\cos E\right)^{-1}dt + d\sigma_E \qquad (2)
$$

where $\sigma_E$ –the variation of the rate of change of the eccentric anomaly in the perturbed motion. It is determined from the equation of the Kepler:

$$
d\sigma_E = \frac{\sin E}{1-e\cdot\cos E}de - \frac{3}{2}\cdot\frac{t-\tau}{1-e\cdot\cos E}dw\sqrt{\frac{\mu}{w^6}} - \frac{t}{1-e\cdot\cos E}\sqrt{\frac{\mu}{w^3}}d\tau \qquad (3)
$$

where $\tau$ – the passage of the perigee. After transformation, we have:

$$
\begin{aligned}
\frac{dp}{dE} &= 2\frac{p^3}{\mu\left(1-e^2\right)^{2.5}}w\sin\lambda(1-e\cdot\cos E)^2\cdot\xi \\
\frac{de}{dE} &= \frac{p^2 w}{\mu\cdot\left(1-e^2\right)^{1.5}}\left(\begin{aligned}&\cos\lambda\sin E\sqrt{1-e^2}+\\&+\sin\lambda(2\cos E-e-e\cdot\cos^2 E)\end{aligned}\right)\cdot\xi \\
\frac{dr_\pi}{dE} &= \frac{p^3 w}{\mu\cdot\left(1-e^2\right)^3}\left(\begin{aligned}&\sqrt{\frac{1-e}{1+e}}\sin\lambda\left[\begin{aligned}&2(1-e\cos E)^2-\\&-(1-e)(2\cos E-e-e\cos^2 E)\end{aligned}\right]-\\&-\cos\lambda\sin E(1-e)^2\end{aligned}\right)\cdot\xi
\end{aligned}
\qquad (4)
$$

where

$$
\xi = \left(1+\sqrt{\frac{p^3}{\mu\cdot\left(1-e^2\right)^3}}\cdot\left(1-e\cdot\cos E\right)\cdot\frac{d\sigma_E}{dt}\right)^{-1} \qquad (5)
$$

Considering the assumption of the smallness of the thrust acceleration, we neglect the terms containing $w^2$ in (3) and (5). We obtain, that $\xi = 1$.

In (4) $r_{\pi}$ – is the radius of perigee of the orbit. It may be replaced by the altitude of the perigee $H_{\pi}$, according to the formula $r_{\pi} = H_{\pi} + R$, where $R$ – is the average radius of the Earth (6371 km).

*B. The Locally - Optimal Control Program*

We define the locally optimal control program of the orientation of the trust angle $\lambda_{lok}$. It will provide the greatest rate of the change of the radius of the perigee $r_{\pi}$. For that we find the solution of the equation $\frac{\partial}{\partial\lambda}\frac{dr_{\pi}}{dE} = 0$ concerning to the control parameter $\lambda$ [17].

$$\tan\lambda(E)_{lok} = \pm\frac{2(1-e\cdot\cos E)^2 - (1-e)(2\cos E - e - e\cos^2 E)}{\sin E(1-e)\sqrt{1-e^2}} \quad (6)$$

*C. The Optimal Control Program*

Let us estimate the maximal possibilities of the control of the perigee on the orb. For that, we use the Pontryagin maximum principle [18]. For the same assumptions, we define the optimal control program of the orientation of the trust angle $\lambda_{opt}$.

In accordance with the general algorithm of the maximum principle, we write the Hamiltonian of the system (4) with the criterion $r_{\pi} \to \min$:

$$H = \psi_p \cdot \frac{dp}{dE} + \psi_e \cdot \frac{de}{dE} + \psi_E - \frac{dr_{\pi}}{dE} \quad (7)$$

where $\Psi = (\psi_p, \psi_e, \psi_E)$ –is the vector of the Lagrange multipliers. Factor $\psi_E$ takes into account the not autonomous of the system (4). Substituting the right-hand sides of equations (4) to (7), we obtain:

$$\begin{aligned}
H = {} & 2\cdot w\cdot\psi_p \cdot \frac{p^3}{\mu\cdot(1-e^2)^{2.5}}\cdot(1-e\cos E)^2\cdot\sin\lambda + \\
& + w\cdot\psi_e \cdot \frac{p^2}{\mu\cdot(1-e^2)^2}\cdot\begin{bmatrix}\cos\lambda\cdot\sin E\sqrt{1-e^2} + \\ +\sin\lambda\cdot(2\cos E - e - e\cdot\cos^2 E)\end{bmatrix} - \\
& -\frac{p^3}{\mu\cdot(1-e^2)^3}\cdot w\cdot\begin{pmatrix}\sqrt{\frac{1-e}{1+e}}T\begin{bmatrix}2(1-e\cos E)^2 - \\ -(1-e)(2\cos E - e - e\cos^2 E)\end{bmatrix} - \\ -S\cdot\sin E\cdot(1-e)^2\end{pmatrix}
\end{aligned} \quad (8)$$

Optimal control is determined from the condition of the maximum of the Hamiltonian. It stationary condition has the form $\frac{dH}{d\lambda} = 0$.

Value of the angle $\lambda_{opt}$, satisfying the condition of the stationarity, has the form:

$$\begin{aligned}
\tan\lambda_{opt}(E) = {} & \frac{(2\cos E - e - e\cos^2 E)\left[\psi_e\sqrt{1+e} + \frac{p}{(1+e)^{1.5}}\right]}{\sin E\cdot\sqrt{1-e}\left[\psi_e(1+e) + \frac{p}{1+e}\right]} + \\
& + \frac{2p\frac{(1-e\cdot\cos E)^2}{1-e^2}\left[\psi_p\sqrt{1+e} - \frac{1}{\sqrt{1+e}}\right]}{\sin E\cdot\sqrt{1-e}\left[\psi_e(1+e) + \frac{p}{1+e}\right]}
\end{aligned} \quad (9)$$

The equation for the conjugate multipliers takes the form:

$$\begin{aligned}
\frac{d}{dE}\psi_p = {} & -\frac{\partial H}{\partial p} = -6w\psi_p\frac{p^2}{\mu}\frac{(1-e\cdot\cos E)^2}{\left(1-e^2\right)^{2.5}}\sin\lambda - \\
& -2w\psi_e\frac{p}{\mu\cdot\left(1-e^2\right)^{1.5}}\cdot\begin{bmatrix}\cos\lambda\sin E\sqrt{1-e^2} + \\ +\sin\lambda(2\cos E - e - e\cdot\cos^2 E)\end{bmatrix} + \\
& +3w\frac{p^2}{\mu\left(1-e^2\right)^3}\begin{pmatrix}\sqrt{\frac{1-e}{1+e}}\sin\lambda\begin{bmatrix}2(1-e\cos E)^2 - \\ -(1-e)(2\cos E - e - e\cos^2 E)\end{bmatrix} - \\ -\cos\lambda\sin E(1-e)^2\end{pmatrix}
\end{aligned} \quad (10)$$

$$\begin{aligned}
\frac{d}{dE}\psi_e = {} & -\frac{\partial H}{\partial e} = -2w\psi_p\frac{p^3}{\mu}\begin{pmatrix}5e\cdot\frac{\left(1-e\cdot\cos^2 E\right)^2}{(1-e^2)^{3.5}} - \\ -\frac{2\cdot\cos E\cdot(1-e\cdot\cos E)}{(1-e^2)^{2.5}}\end{pmatrix}\sin\lambda - \\
& -\psi_e\frac{p^2}{\mu}w\begin{bmatrix}\sin\lambda\frac{3e\left(2\cos E - e - e\cos^2 E\right)}{\sqrt{1-e^2}} - \\ -\frac{\left(1-e^2\right)\left(1+\cos^2 E\right)}{\sqrt{1-e^2}} + 2e\sin E\cos\lambda\end{bmatrix} - \\
& \frac{p^3}{\mu(1-e^2)^3}w\left\{\begin{array}{l}\frac{6e}{1-e^2}\begin{pmatrix}\sin\lambda\sqrt{\frac{1-e}{1+e}}\begin{pmatrix}2(1-e\cos E)^2 - \\ -(1-e)\times \\ \times(2\cos E - e - e\cos^2 E)\end{pmatrix} - \\ -\cos\lambda\sin E(1-e)^2\end{pmatrix} + \\ +\sin\lambda\sqrt{\frac{1-e}{1+e}}\begin{pmatrix}-4\cos E\cdot(1-e\cdot\cos E) + \\ +2\cos E - e - e\cos^2 E + \\ +(1+e)(1+\cos^2 E)\end{pmatrix} - \\ -\sqrt{\frac{1+e}{1-e}}\frac{\sin\lambda}{(1+e)^2}\begin{pmatrix}2(1-e\cos E)^2 - \\ -(1-e)\times \\ \times(2\cos E - e - e\cos^2 E)\end{pmatrix} - \\ -\cos\lambda\sin E(1-e)^2\end{array}\right\}
\end{aligned} \quad (11)$$

*D. The Boundary Value Problem*

The values of the conjugate multipliers $\psi_{p_\kappa}, \psi_{e_\kappa}$ must be equal to zero at the end point of the orbital transfer $E = \pi\cdot n, n \in N$. Then the boundary conditions of the solved system (4), (10) and (11) subject to the control (9) takes the form:

$$E=0: p=p_0,\ \ e=e_0,$$
$$E=E_f: \psi_{p_f}=0, \psi_{e_f}=0\ , \tag{12}$$

where the index "f" is mean the end point of the orbital transfer.

The boundary value problem reduces to the determine of the initial values of the conjugate multipliers $\psi_{p0}, \psi_{e0}$ for satisfy the boundary conditions (12). Boundary value problem has a good convergence upon the integration from the endpoint to the primary point with a negative step.

For that we use solutions, calculated using the locally – optimal control program

*E. The Resistance of the Atmosphere*

After disconnection from the SDC the fragment of the SD makes does not perturbed orbital motion. At the altitudes below 1,500 km the fragment of the SD begins the deceleration due to the atmospheric drag. Atmosphere reports the acceleration to the fragment of the SD. By the nature, the atmospheric acceleration directed against of the velocity vector. It can described by the formula:

$$\overrightarrow{w_a}=-\frac{C_x \cdot F_m}{2 \cdot m} \cdot \rho \cdot V^2 \cdot \overrightarrow{V^0} \tag{13}$$

where $c_x$ – is the dimensionless atmospheric drag coefficient, $F_m$ – the area of the middle section of the fragment of the SD, $m$ – mass of the fragment of SD, $\rho$ – the density of the atmosphere, $V$ – the velocity of the fragment of SD, $\overrightarrow{V^0}$ – unit velocity vector.

The atmospheric density is determined in accordance with the standard [17]. It depends from the level of the solar activity *F*. Calculations will performed for the averaged values of the solar activity level: $F=175 \cdot 10^{-22} \frac{\text{W}}{\text{m}^2 \cdot \text{Hz}}$.

Projections of the atmosphere disturbance acceleration on the orbital coordinates frame will defined as:

$$w_{a_x}=-w_a\sqrt{\frac{1-e^2}{1-e^2\cos^2 E}} \tag{14}$$

$$w_{a_y}=-w_a\frac{e\sin E}{\sqrt{1-e^2\cos^2 E}} \tag{15}$$

## III. Numeric Simulations

*A. Numeric Simulation of the Optimal and the Locally Optimal Control Programs for an Arbitrary Orbit*

We consider an orbital transfer between an arbitrary orbits with parameters: the radius of the perigee $r_\pi=26371\,km$, radius of apogee $r_\alpha=36371\,km$, the focal parameter $p=30574\,0\,km$ and the eccentricity $e=0.159$. The fig. 2 display the optimal and the locally - optimal control programs within the orb as a functions of the angle of the eccentric anomaly *E*.

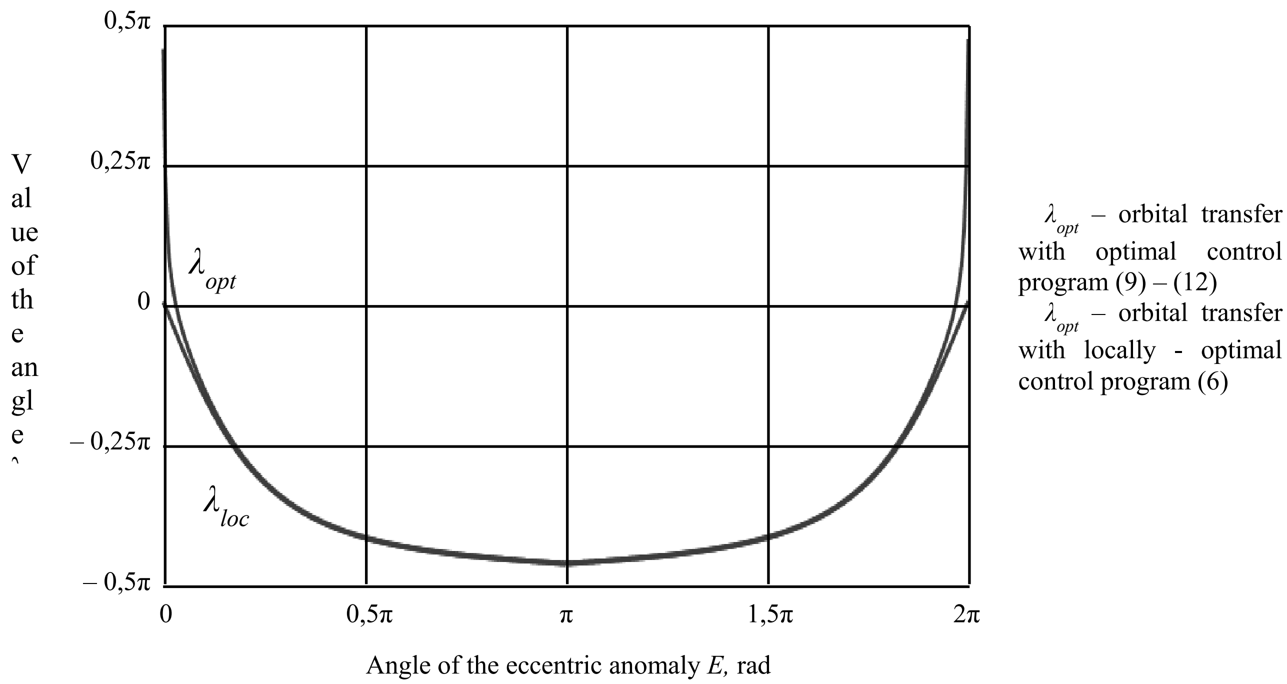


Fig. 2. The optimal and the locally - optimal control program on the orbit as function of the angle of the eccentric anomaly *E*

As follows from the obtained results (see fig. 2), the optimal and the locally - optimal thrust vector control programs for the selected optimality criterion similar despite a significant mismatch programs at the perigee point.

Let us estimate the efficiency of the received control programs. For that we integrate the system (4) with the locally - optimal program (6), next with the optimal control program (9) taking into account the conjugate multipliers (10) – (11) and the boundary conditions (12). We considered a single-turn and a multi-turn orbital transfers (30 orbs). The calculation is performed for thrust acceleration $w = 1\ mm/s^2$. The results (the final value of the radius of the radius of the perigee) are shown in Table 1. In the third column of the Table 1 we show the gains of using of the optimal control program, such as a percentage of the final values of the radius of perigee, obtained using the locally – optimal control program.

*B. Determination of the Elliptical Orbits, which can be Used for the Descent of the fragment of the SD (the Release Orbits)*

Let us consider the feasibility of the obtained control programs for the proposed scheme of the descent of the fragment of the SD from elliptical orbit. For that, we integrate system (4) with control program (6) on the range of the eccentric anomaly $E \in \{0, \pi\}$ for different values of the thrust acceleration *w*. We pose the problem of the reducing of the height of the perigee of 100 km such a way that the fragment of the SD was guaranteed captured atmosphere in the pericenter. At the same time SDC should raise height of perigee to the required values (200 km).

We introduce into consideration parameter $\chi$:

$$\chi = \frac{m_d}{m_{SDC}} \tag{16}$$

where $m_d$ – the mass of fragment of SD, $m_{SC}$ – the mass of the SDC.

Then the thrust acceleration of the SDC after separation the fragment of the SD $w_2$ will calculated as follows:

$$w_2 = \frac{w_1\left(m_d + m_{SDC}\right)}{m_{SDC}} = w_1\left(1+\chi\right) \tag{17}$$

Thereby movement of the SDC will occur with different acceleration: at the first part of the orb, it will less, at the second part of the orb it will greater. The fragment separation point can moved forward from the point of the apocentre. It improve the conditions for the descent of the fragment of the SD.

We define the values of the initial heights of the apogee $H\alpha^*$ and the values of the eccentric anomaly $E^*$, in which we separate the fragment of the SD, providing care of the SDC to the clearance height. The results of calculation $H\alpha^*$ for different values of the acceleration $w$ and $\chi$ represent at the figure 3.

TABLE I
THE COMPARISON OF THE CONTROL PROGRAMS

| The duration of the orbital transfer | The height of the perigee at the end of the orbital transfer, km | | The gains of using of the optimal control program (the greater decreasing of the height of the perigee) |
|---|---|---|---|
| | The locally - optimal control program | The optimal control program | |
| One orb | 25514 | 25511 | about 0,1 % |
| Thirty orbs | 17782 | 16929 | greater to 5 – 7 % |

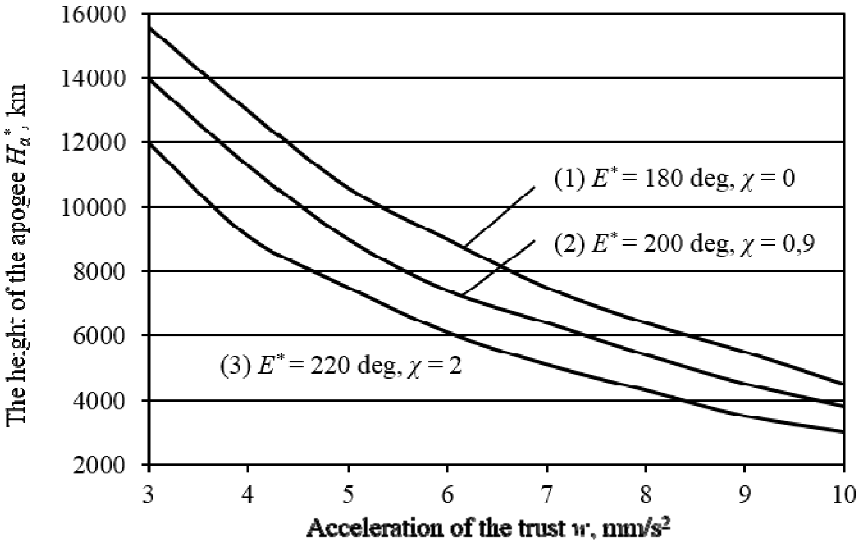


1 – the ideal case, the mass of the fragment of the SD is equal to zero (SDC have not extra acceleration (17) to return to the initial orbit)

2 – the mass of the fragment of the SD greater of the mass of the SDC in 0,9 times, point of the disconnection is $E$ = 220 deg

3 – the mass of the fragment of the SD greater of the mass of the SDC in 2 times, point of the disconnection is $E$ = 220 deg

Fig. 3. The results of calculation $H\alpha^*$ for different values of the acceleration $w$ and $\chi$

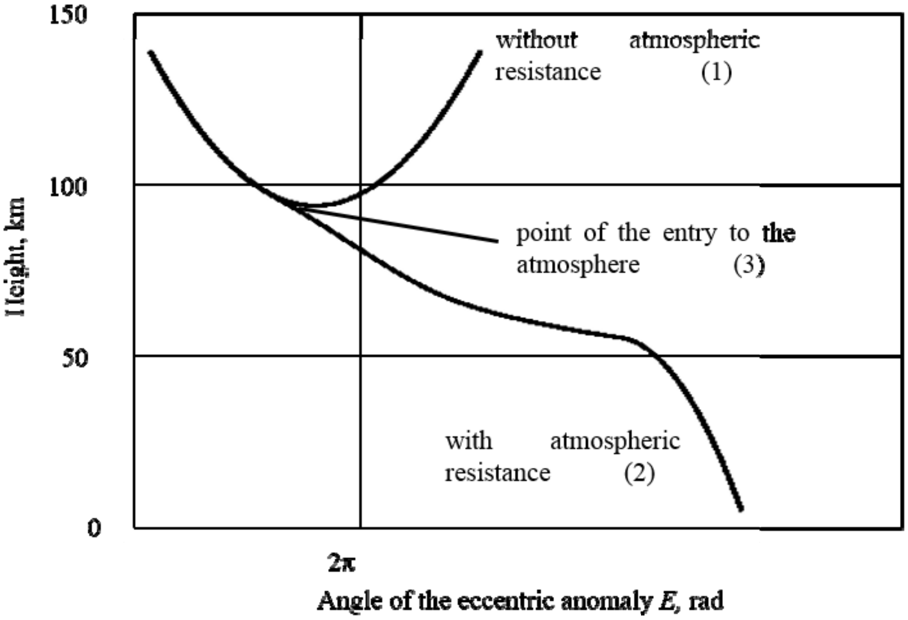


**1 – this line is corresponded to the Keplerian orbital motion of the fragment of the SD without atmospheric perturbations (area to mass ratio $\sigma_x = 0$)**

**2 – this line corresponded to the motion of the fragment of the SD with atmospheric perturbations. At the height 90– km (for this Release orbit) the fragment of the SD is entrance to the Earth atmosphere and landing to it's surface**

**3 – the point of the entrance of the fragment of the SD to the Earth atmosphere (for details, see section III.D)**

Fig 4. Reducing of the fragment of the SD with the ballistic coefficient 0.004 m$^2$/kg in the Earth's atmosphere

Examining the Fig. 3 we can conclude, that it is possible to dispose the fragments of the SD having the following numbers in the NORAD database: ID 16993, ID 23420, ID 22671, ID 15952 and other. The height of the apogee of this fragments of the SD is 12 .. 16 thousands km.

*C. Descent from the Elliptical Orbit*

Let us carry out checking calculations. We show that the fragment of the SD after separation from the SDC reaches the Earth's surface in the area of pericenter. We introduce into consideration parameter of the height of the fragment of the SD:

$$h = \frac{p \cdot (1 - e \cdot \cos E)^2}{1 - e^2} - R \qquad (18)$$

where $R$ – the average radius of the Earth (6371 km).

We integrate the system (4) with the acceleration (13) for the fragment of the SD with the area to mass ratio 0,004 m$^2$/kg (it mean as average). Consider the descent from the orbit with parameters $r_\pi = 90\,km, r_\alpha = 15599\,km$ .The trajectory of the fragment of SD on the second semi orb on the area of the strong influence of the atmosphere is represent at the fig. 4.

In the course of the simulation is set, that the capture of fragment of the SD in the atmosphere take place at the altitudes about 90..110 km.

Analyzing the motion trajectories of the fragment of the SD in the upper atmosphere of the Earth, we can conclude that the fragments of the SD guaranteed reach the Earth's surface and does not continue existence in the near-Earth space.

*D. Angle of Entry to the atmosphere*

Let us calculate some extra parameters of the motion of the SD at the moment of the entrance to the Earth atmosphere.

In previous section we calculate, that the fragment of the SD enters to the Earth's atmosphere and reaches the Earth's surface. In this section we will clarify parameters of the entrance of the fragment of the SD to the atmosphere. One of the most important parameter of the entrance to the atmosphere is the angle of the entrance. For elliptical orbit this angle can be determined as angle between vector of the orbital velocity of the fragment of the SD and the line of the local horizon (i.e. the normal to the moment radius – vector in orbital frame $r$ (see fig.1)).

For that purpose we use the velocity coordinate system instead of the system of the osculating elements (1).

$$m\frac{dV}{dt} = -C_{xa} S_m \frac{\rho \cdot V^2}{2} - mg\sin\theta,$$
$$mV\frac{d\theta}{dt} = -C_{y_a} S_m \frac{\rho \cdot V^2}{2} + \frac{mV^2}{R+h}\cos\theta - mg\cos\theta,$$
$$\frac{dh}{dt} = V\sin\theta,$$

where $m$ – the mass of the SD, $V$ – the orbital velocity of the SD, $C_{xa}$ – dimensionless coefficient of the aerodynamic resistance of the SD, $C_{ya}$ – dimensionless coefficient of the lifting force (for the spherical body is equal to zero), $S_m$ – the area of the middle section of the fragment of the SD, $\rho$ – the density of the atmosphere, $g$ – the acceleration of the Gravity, $\theta$ – the angle of the inclination of the trajectory, $h$ – geocentric height, $R$ – the average radius of the Earth.

The acceleration of the Gravity describes by formula:

$$g(h) = g_0 \left( \frac{R}{R+h} \right)^2,$$

where $g_0$ – the acceleration of the Gravity at the Earth surface (is equal to 9,806 m/s$^2$).

After dividing the first two equations of the system (19) to the mass, we obtain:

$$\begin{aligned} &\frac{dV}{dt} = -\sigma_x \cdot \rho \cdot V^2 - g \cdot \sin\theta, \\ &V \cdot \frac{d\theta}{dt} = \frac{V^2}{R+h} \cdot \cos\theta - g \cdot \cos\theta, \\ &\frac{dh}{dt} = V \cdot \sin\theta, \end{aligned} \qquad (21)$$

where $\sigma_x -$ the area to mass ratio of the fragment of the SD. We use average value of this coefficient, equal to 0,004 $\mathrm{m}^2/\mathrm{kg}$ , as well as in section III.C.

We integrate system (21) from the moment where the fragment of the SD passed the apocenter of the elliptical orbit and we stop integration at moment *t*, corresponded to the moment of the landing of the fragment of the SD to the Earth's surface.

The initial value of the height (the third equation of the system (21)) assumed to be equal to the radius of the apogee of the orbit of the fragment of the SD. The speed of the fragment of the SD in the apocentre of the elliptical orbit can be determinate by formula:

$$V = \sqrt{\frac{\mu}{p}} \cdot (1-e). \qquad (22)$$

In section III.C we calculate the heights of the apogee of the elliptical Release orbits. In table 2 we show calculated angle of the entrance to the Earth atmosphere for every elliptical Release orbit.

TABLE II
THE ANGLE OF THE ENTRANCE OF THE FRAGMENT OF THE SD TO THE EARTH ATMOSPHERE AT THE ALTITUDE 100 KM FOR THE VARIOUS ELLIPTICAL RELEASE ORBITS

| № | The angle of the entrance to the atmosphere, deg | The height of the apogee of the elliptical Release orbit, km |
|---|---|---|
| 1 | – 2,62 | 15599 |
| 2 | – 2,47 | 13888 |
| 3 | – 2,37 | 12309 |
| 4 | – 2,3 | 11317 |
| 5 | – 2,25 | 10314 |
| 6 | – 2,18 | 8677 |
| 7 | – 2,06 | 7383 |
| 8 | – 1,92 | 6417 |
| 9 | – 1,83 | 5866 |
| 10 | – 1,72 | 5441 |
| 11 | – 1,62 | 5049 |
| 12 | – 1,56 | 4755 |

From table 2 we can conclude, that the angle of the entrance to the atmosphere increase (in absolute value) with increasing of the eccentricity of the elliptical Release orbit.

Let us study the dynamic of the angle of the inclination of the trajectory of the fragment of the SD. We assume, that we use Release orbit with number 6 (see table 2). At figure 5, we show the graph of the angle of the INCLINATION of the trajectory of the fragment of the SD on all orbit, at figure 5a we show the angle of the ENTRANCE of the fragment of the SD to the atmosphere.

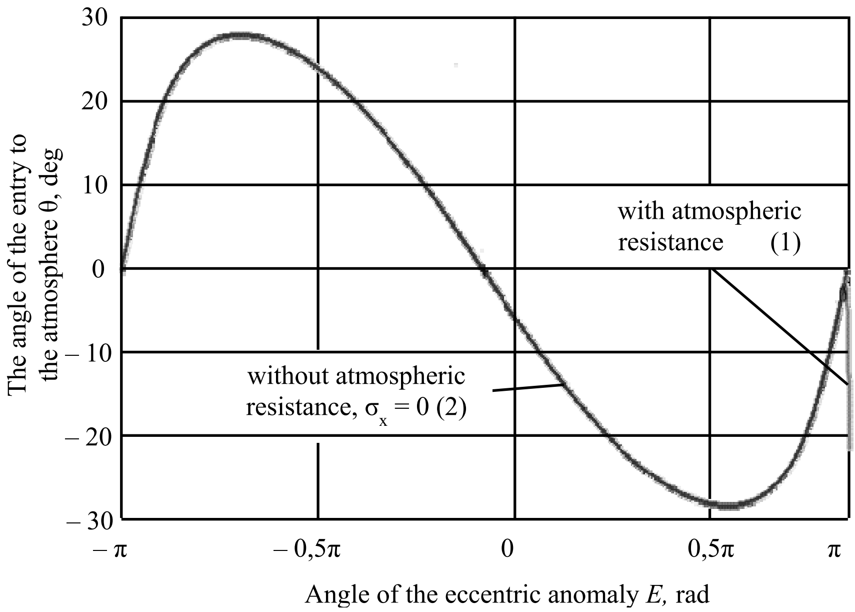


1 – this line corresponded to the motion of the fragment of the SD with atmospheric perturbations. The angle of the ENTRANCE of the fragment of the SD limit to –90 deg, that mean the landing of the fragment of the SD to the Earth surface

2 – this line is corresponded to the Keplerian orbital motion of the fragment of the SD without atmospheric perturbations (area to mass ratio $\sigma_x$ = 0). The function of the angle of the INCLINATION of the trajectory is periodic.

Fig. 5. The angle of the entrance to the atmosphere of the fragment of the SD at elliptical Release orbit number 6 (see table 2) at all orbit. The line, which corresponded to atmospheric resistance aimed to the value $\theta$ equal to – 90 deg (it mean landing to the Earth surface). The second line is corresponded to motion without atmospheric perturbations (does not perturbation Keplerian motion)

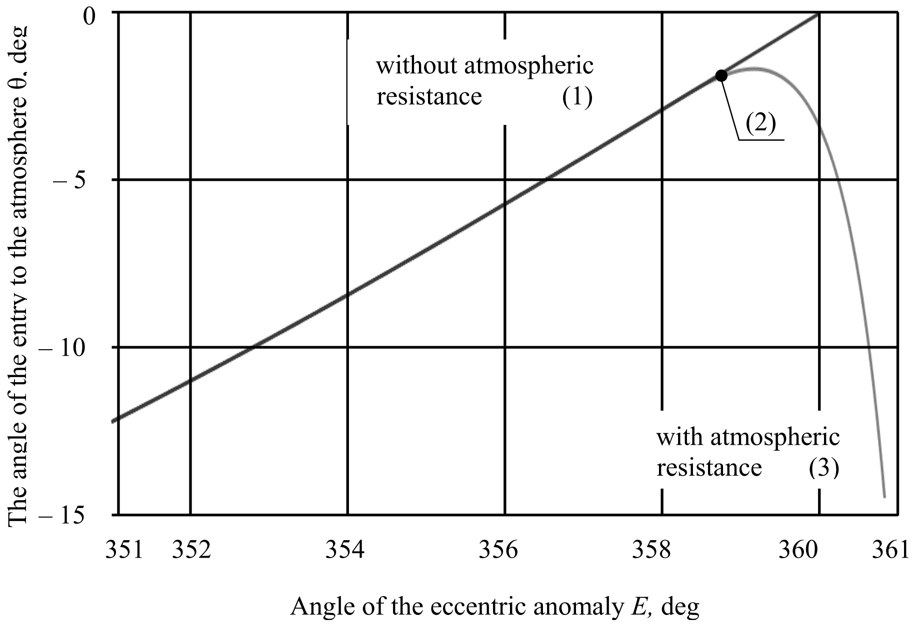


1 – this line corresponded to the motion without atmospheric resistance. The angle of the INCLINATION of the trajectory is limit to 0 deg.
2 – the point of the entrance of the fragment of the SD to the Earth atmosphere. In this point the angle of the inclination of the trajectory have start to limit to the –90 deg
3 – the graph of the angle of the ENTRANCE of the fragment of the SD to the atmosphere

Fig. 5a. The angle of the entrance to the atmosphere of the fragment of the SD at elliptical Release orbit number 6 (see table 2) in area of the strong influence of the Earth atmosphere

From figure 5a we can conclude, that the process of the entrance of the fragment of the SD to the atmosphere is very quickly. It's duration is only 1 – 2 deg of the eccentric anomaly. The point of the entrance of the fragment of the SD to the atmosphere can be determined as point of the inflection of the graph of the angle of the inclination of the trajectory of the fragment of the SD.

Thus, the angle of the inclination of the trajectory becomes to the angle of the entrance to the atmosphere (the last is increase (in absolute value)).

We calculate the value of the angle of the entrance of the fragment of the SD to the atmosphere for minimal fixed value of the solar activity level, prescribed by the standard [19]. Therefore, for the minimal value of the atmospheric acceleration (13). With increasing of the solar activity level, the atmospheric acceleration will increase as well as the angle of the entrance to the atmosphere.

*E.* The track of the fragment of the SD

Another important aspect in the problem of disposal of the SD is to provide the landing of the fragments of the SD in the predetermined area of the Earth's surface. In accordance with standard [6] all of the spacecraft, after the end of life, must be disposal in the South of the Pacific Ocean.

In previous sections, we calculate the characteristics of the elliptical Release orbits. Now we simulate the track of the fragment of the SD at the motion on the elliptical Release orbit. Geographic latitude and longitude of each point of the track of the fragment of the SD can be found by the formulas:

$$\alpha = \arctan(\tan u \cdot \cos i) - \omega_E (t - t_0) + \delta\Omega \frac{t - t_0}{T},$$
$$\delta = \arcsin(\sin u \cdot \sin i), \qquad (23)$$

where $\delta\Omega$ – the secular shift of the longitude of the ascending node, $u$ – the argument of the latitude, $u = \omega + \vartheta$, $\omega$ – the argument of the perigee, $\vartheta$ – the angle of the true anomaly, $i$ – the inclination of the orbit, $\omega_E$ – the angular velocity of the Earth $\left(7{,}29 \cdot 10^{-5}\ \frac{\text{rad}}{\text{s}}\right)$, $T$ – the period of the revolution of the fragment of SD on the orbit, $t - t_0$ – time, in this case, calculated from the moment of the passage of the perigee.

We assume that the inclination of the orbit is constant and equal to 51 deg. The initial value of the longitude of the ascending node was chosen with ensure to provide the landing of the fragment of the SD in the South of the Pacific Ocean.

The value of the argument of the perigee $\omega$ can be founded with joint integration of the system of equations (4) with equation:

$$\frac{d\omega}{dE} = \frac{wp^2}{e\mu\left(1 - e^2\right)^{1.5}} \cdot \left( \sin\lambda \frac{\sin E\left(2 - e^2 - e\cos E\right)}{\sqrt{1 - e^2}} - \cos\lambda\left(\cos E - e\right) \right).$$

The initial value of the argument of the perigee was chosen as value of the $\Omega$.

The angle of the true anomaly $\vartheta$ is corresponded with the angle of the eccentric anomaly $E$ by formula:

$$\frac{d\vartheta}{dE} = \frac{\sqrt{1 - e^2}}{1 - e\cos E}.$$

We simulate the track of the fragment of the SD for all elliptical Release orbits. At figure 6, we show the track of the fragment of the SD for the elliptical Release orbit number 1 (see table 2). We simulate the daily track with taking into account the rotation of the Earth.

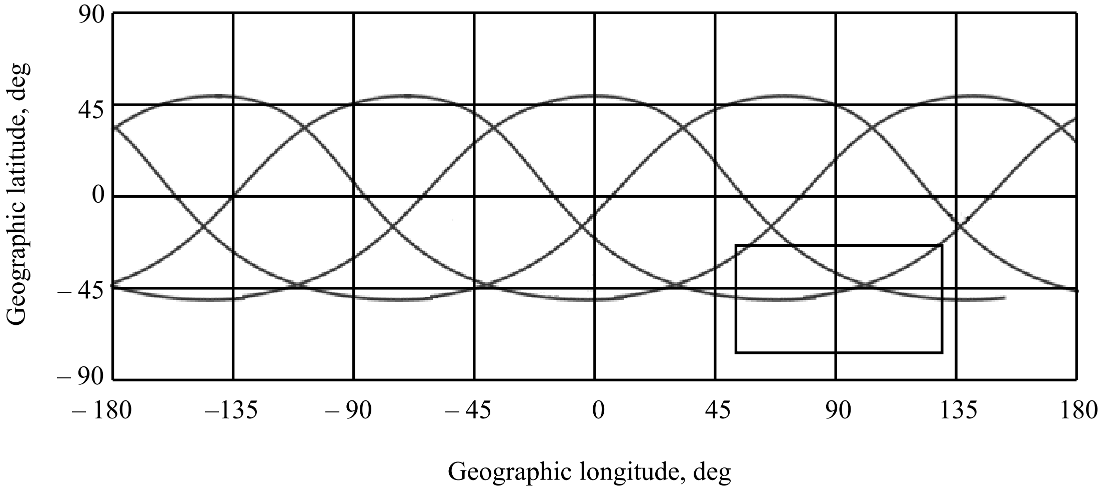


Fig. 6. The track of the fragment of the SD for the elliptical Release orbit number 1 (see table 2)

At figure 6, we show in rectangular the South of the Pacific Ocean. We chose the value of the longitude of the ascending node $\Omega = -60\,\text{deg}$ and the value of the argument of the perigee $\omega = -80\,\text{deg}$.

We simulate the track for other elliptical Release orbits (see table 2) and we have similar result for the initial values of the longitude of the ascending node and for the argument of the perigee.

During the day, the pericenter of the elliptical Release orbit passes only once over the South of the Pacific Ocean. From that we can conclude, that any mistake (such as transfer of the SDC to an unplanned orbit) in control of the SDC will have place, so the process of the disposal of the fragment of the SD will be postponed for a day, which could lead to a threat of collision with other spacecraft and other undesirable consequences

*F. Descent from the Circular Orbit*

Let us study descent of the fragments of the SD with the SDC from the circular Release orbit. To increase the accuracy of the forecast point of landing of the fragment of the SD on the Earth's surface we can use a low-thrust propulsion of the engines of the SDC. Thus, we can reduce the number of the revolutions, which passed the fragment of the SD, before it is entering to the Earth's atmosphere in the uncontrolled mode (the mode of self-locking).

We simulated the descent of the fragment of the SD from the circular Release orbits with different heights in the mode of self-locking. After delivery of the fragments of the SD to these orbits, SDC moves to the safe orbit and the fragment of SD start descent.

To determine the number of revolutions, which passed the fragments of the SD around the Earth, we integrate the system (4) with acceleration (13), which project to axes of orbital frame as (14) and (15). Result is shown at fig. 7.

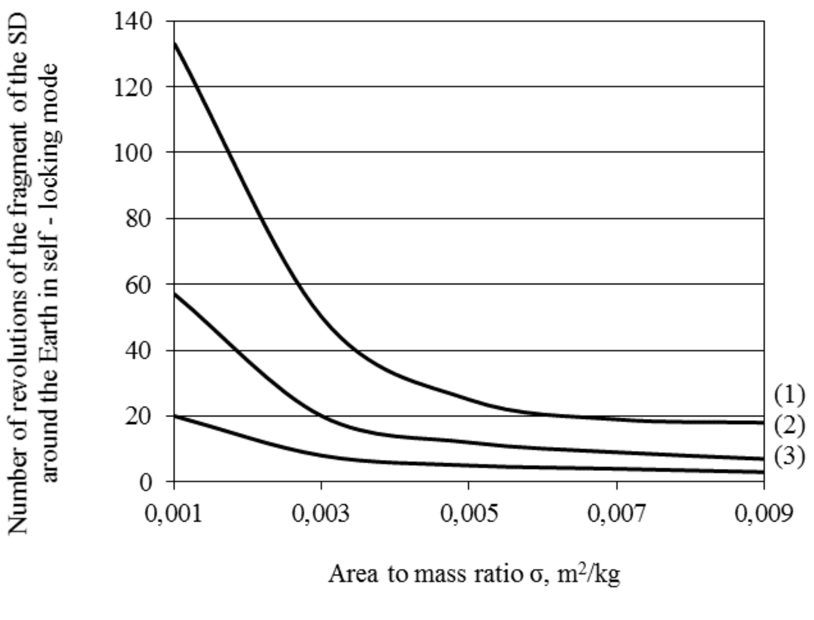


The descent of the fragment of the SD from the initial circular Release orbit in self-locking mode due to the acceleration from the atmospheric resistance (13) and it's projections to the axis of the orbital frame (14) and (15).

1 – the height of the circular Release orbit is 200 km

2 – the height of the circular Release orbit is 180 km

3 – the height of the circular Release orbit is 160 km

Fig. 7. Number of revolutions, passed the fragment of the SD, in self-locking mode at descent from different circular orbits

These results demonstrate, that reducing of the height of the release circular orbit from 200 to 180 km, can significantly (several times) reduce the number of the revolutions around the Earth, passed the fragment of the SD in the uncontrolled mode.

## IV. Calculation of the Characteristic Velocity, Required to Delive the Fragments of the SD to the Release Orbits

We have calculated the gains of the characteristic velocity required to deliver the fragment of the SD to the Release elliptical and circular orbits.

### A. Formation of the Elliptical Release Orbit

Let us study the problem of formation of the elliptical Release orbit with the height of perigee of 200 km, which used to implement the controlled descent of the fragment of the SD using low-thrust.

We ranged the height of the perigee $H_\pi$ and the height of the apogee $H_\alpha$ of initial orbit (the fragment of the SD is located on this orbit). We calculate the gains of the characteristic velocity $V_x$, which provide the orbital transfer from the initial orbit to the Release orbit, using locally – optimal program (6):

$$\frac{dV_x}{dE} = w \cdot \sqrt{\frac{p^3}{\mu \cdot \left(1-e^2\right)^3}} \cdot \left(1 - e \cdot \cos E\right) \qquad (19)$$

The results of some calculations are presented at fig. 8 in the form of lines of the equal gains values of $V_x$.The calculation is performed for the thrust acceleration $w = 0{,}1\ \text{mm/s}^2$ .

In this case the level lines is out to be close to a linear functions.

### B. Formation of a Circular Release Orbit

We calculated the costs of the characteristic velocity, necessary for controlled delivery of the fragment of the SD from the circular initial orbit with height 200 km to the Release orbit with height 180 and 160 km. Soon after that, for return of the SDC to the initial orbit.

The calculation is performed for the thrust acceleration $w = 2\,mm/s^2$ .

Calculation results are presented at fig. 9a and 9b. Fig. 9a shows the calculation of the characteristic velocity for option to reduce the height of initial orbit 180 km and return back, fig. 9b - to the height of initial orbit 160 km and return back.

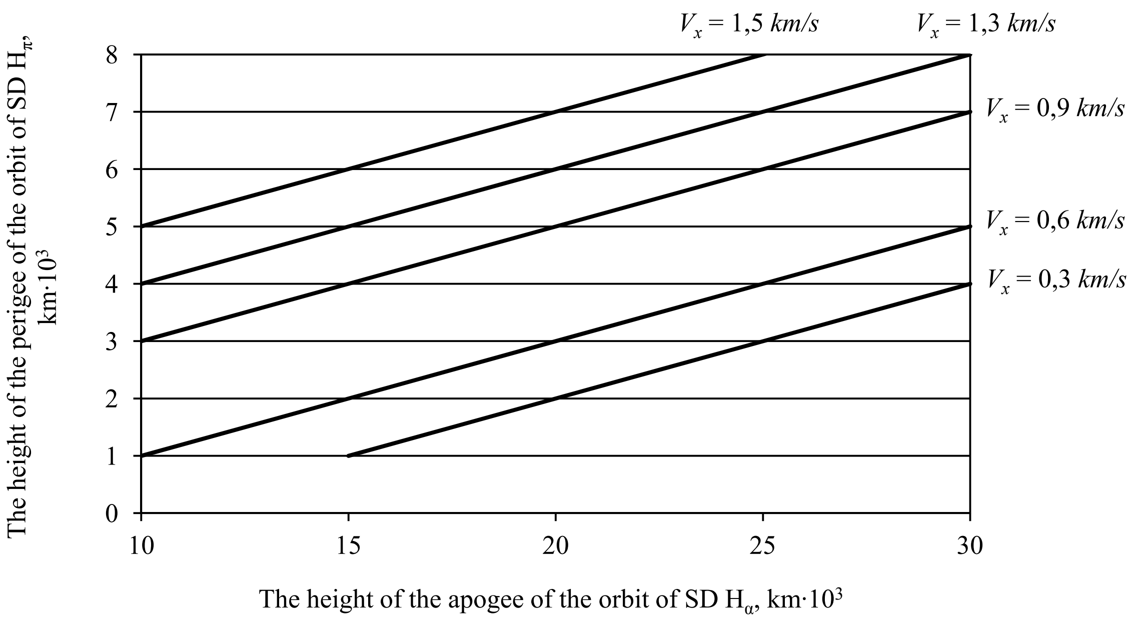


Fig. 8. The gains of the characteristic velocity for transfer SDC and fixed the fragment of the SD from the initial to release orbit

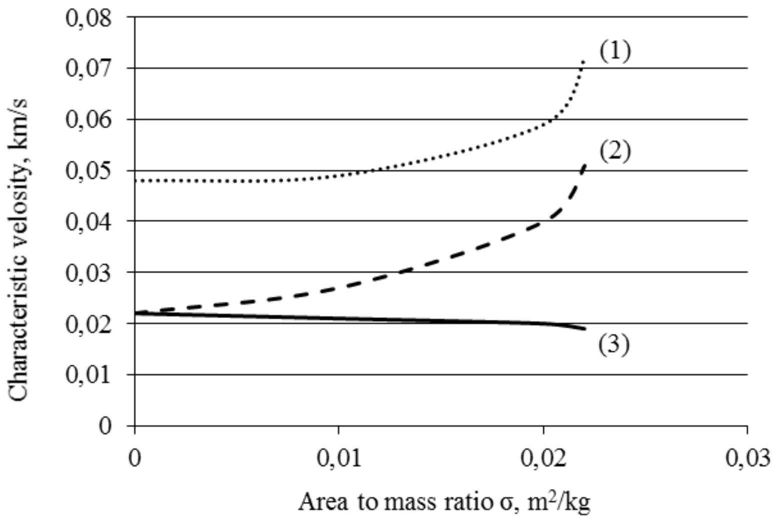


The gains of the characteristic velosity for the descent of the SDC with various area to mass ratio:
1 – for the descent from the initial circular orbit with height 200 km to the circular Release orbit with height 180 km
2 – to return to the initial orbit
3 – the total gains of the characteristic velocity of the orbital transfer

Fig. 9a. The gains of characteristic velocity for reduction circular release orbit of height of 180 km

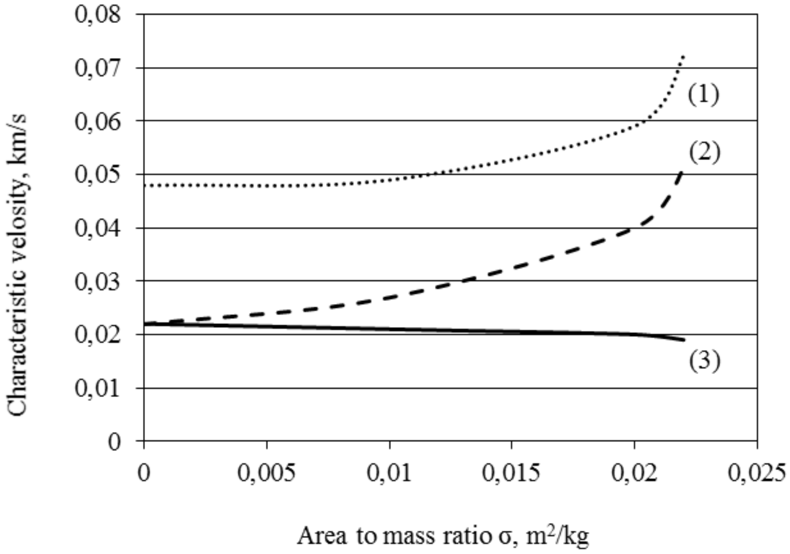


The gains of the characteristic velosity for the descent of the SDC with various area to mass ratio:
1 - for the descent from the initial circular orbit with height 200 km to the circular Release orbit with height 160 km
2 - to return to the initial orbit
3 - the total gains of the characteristic velocity of the orbital transfer

Fig. 9b. The gains of characteristic velocity for reduction circular release orbit of height of 160 km

At fig. 8a and 8b, the solid line corresponds to the gains of characteristic velocity to the reduction the SDC and the fragment of the SD from initial orbit to Release orbit. Dotted line corresponds to return of the SDC from the Release orbit to the initial orbit and the point line corresponds to the total gains of the characteristic velocity to perform the operation.

As can be seen from the figures 8a and 8b, the return of the SDC to the initial orbit is the most expensive part of descent operation.

It should be note, that gains of the characteristic velocity grow up slowly and with increasing of the area to mass ratio it is quickly grow up. It explained by the fact, that the acceleration of the atmospheric drag approaching to the acceleration of the thrust propulsion of the SDC with increasing of the ballistic coefficient.

Note, that in the case of descent from the circular orbit, the gains of the characteristic velocity is in several times less than the gains of the characteristic velocity during the descent from a circular orbit. However, it should be understood, that the descent from a circular orbit is a lengthy process (tens of revolutions around Earth against 0.5 orbs in the case of the descent from the elliptical orbit). Moreover, in this case, it is impossible to accurately determine the location of the landing of the fragment of the SD on the surface of the Earth.

## V. Conclusion

In this paper we examined the problem of descent of the space debris using the special spacecraft – debris collector with the low-trust. We composed the math model of the plane motion of the spacecraft – debris collector, which taking into account the resistance of the Earth's atmosphere. We obtained the locally – optimal control program of the orientation of the thrust vector. For the criterion of the maximum rate of change of the radius of perigee and using the Pontryagin maximum principle we formulate and solve the problem of determine of the optimal orientation thrust vector control program. Found that at the stage of delivery of space debris in the Earth's atmosphere can be taken locally – optimal control program of the orientation of the thrust vector. The numerical simulation of the motion allowed to define the parameters of the elliptical Release orbits and thrust acceleration values. From these orbits can be carried out the operation of descent of the fragment of the space debris within one orb. We simulated motion of the fragment of the space debris on the area of the entrance to the atmosphere. Established that for the considered initial conditions capture of the fragment of the space debris in the atmosphere at altitudes about 100 km.

## ACKNOWLEDGMENT

The work was supported by the Ministry of education and science of the Russian Federation in the framework of the implementation of the Program of increasing the competitiveness of Samara State Aerospace University (National Research University) among the world's leading scientific and educational centers for 2013 – 2020 years.

## REFERENCES

[1] Liou, J.C., Johnson, N.L., A LEO satellite post mission disposal study using LEGEND. Acta Astronaut. Volume 57, pp. 324 – 329, 2005.
[2] Olympio, J.T., Frouvelle, N, Space debris selection and optimal guidance for removal in SSO with low – thrust propulsion. Acta Astronautica. Volume 99, pp. 263-275 (2014).
[3] Special database, PC product of Google Earths, access www.satellitedebris.net/satellite/spaceobjects.kml/.
[4] NORAD Two-Line Element Sets, access www.celestrak.com/NORAD/elements/.
[5] Klinkrad, H., Beltrami, P., Hauptmann, S., Martin, C., Sdunnus, H., Stokes, H., Walker, R., Wilkinson, J.: The ESA space debris mitigation handbook 2002. Adv. Space Res. Volume 34, pp. 1251–1259, 2004.
[6] GOST R 52925-2008 Space technology: General requirements for space systems to limit technogenic pollution of circumterrestrial space (National Standard of Russian Federation). Standard form. Moscow, 2008, (in Russian).
[7] Lewis, H.G., White, A.E., Crowther, R., Stokes, H.: Synergy of debris mitigation and removal. Acta Astronaut. Volume 81, pp. 62–68, 2012.
[8] Ryden, K.A, Fearn, D.G., End-of-life disposal of satellites using electric propulsion: An aid to migration of the space debris problem. Science and Technology Series. Volume 93, pp. 371-387, 1997.
[9] Pergola P., Ruggiero A., Anrenucci M., Olimpio J., Summerr L. Expanding foam application for active space debris removal system. 62nd International Astronautical Congress 2011 (IAC 2011). Volume 3, pp. 2215-2225, 2011.
[10] Klinkrad, H., Johnson, N.L. Space debris environment remediation concepts. 5th European Conference on Space Debris; Darmstadt; Germany; 30 March 2009 through 2 April 2009.
[11] Aslanov, V.S., Ledkov, A.S., Dynamics of towed large space debris taking into account atmospheric disturbance. Acta Mechanica, Volume 225, Issue 9, pp. 2685 – 2697, 2014.
[12] Aslanov, V.S., Ledkov, A.S.: Dynamics of the Tethered Satellite Systems. Woodhead Publishing Limited, Cambridge, 2012.
[13] Phipps, C.R., Baker, K.L., Libby, S.B., Liedahl, D.A., Olivier, S.S., Pleasance, L.D., Rubenchik, A., Trebes, J.E., George, E.V., Marcovici, B., Reilly, J.P., Valley, M.T.: Removing orbital debris with lasers. Adv. Space Res. Volume 49, pp. 1283–1300, 2012.
[14] Campbell, J.W.: Using Lasers in Space: Laser Orbital Debris Removal and Asteroid Deflection. Air University, Maxwell Air Force Base, Alabama, 2000.
[15] Wilde M., Chua Z.K., Fleischner A. Effects of Multivantage Point Systems on the Teleoperation of Spacecraft Docking. IEEE Transaction on Human – Machine System. Volume 44, pp. 200 – 210, 2014.
[16] Pardini C., Anselmo L. Physical properties and long-term evolution of the debris clouds produced by two catastrophic collisions in earth orbit. Acta Astronautica. Volume 96, pp. 128 – 137, 2014.
[17] Lebedev, V.N., Dynamic of the spacecraft with low-thrust, Academy of Sciences of USSR, Moscow, 1968, (in Russian).
[18] Pontryagin, L.S., Boltyansky, V.G., The mathematical theory of optimal processes, Moscow State University, Moscow, 1976, (in Russian).
[19] GOST R 25645.166 – 2004 Earth upper atmosphere. Density model for ballistic support of flights of artificial earth satellites (National Standard of Russian Federation). Standard form. Moscow, 2004, (in Russian).
[20] Brito, T.P., Celestino C.C., Moraes R.V. A brief scenario about the "space pollution" around the Earth. Journal of physics: conference series. 465(1), 012020, 2013.
[21] Deluca, L.T., Bernelli, F., Maggi, F., Tadini, P., Pardini, C., Anselmo, L., Grassi, M., Pavarin, D., Francescony , A., Branz, F., Chiesa, S., Viola, N., Trushlyakov, V., Belokonov, I. Active space debris removal by a hybrid propulsion module. Acta Astronautica. Volume 91, pp. 20 – 33, 2013.
[22] Tang C., Liu, Y., Gao, Z., Tang, Q., Li, Y. Space debris removal in ultra – closed based on visual navigation. Proceedings of the International Astronautical Congress, IAC 14, pp. 11238 – 11250, 2013.
[23] White, A.E., Lewis, H.G. The many futures of active debris removal. Acta Astronautica. Volume 95, Issue 1, pp. 189 – 197, 2014.
[24] Schaub, H., Sternovsky, Z. Active space debris charging for contactless electrostatic disposal maneuvers. Advances in Space Research. Volume 53, Issue 1, pp. 110 – 118, 2014.
[25] Kitamura, S., Hayakawa, Y., Kawamoto, S. A reorbiter for large GEO debris objects using ion beam irradiation. Acta Astronautica. Volume 94, Issue 2, pp. 725 – 735, 2014.
[26] Rosengren, A.J., Scheerse, D.J., McMahon, J.W. Long-term dynamics and stability of GEO orbits: The primacy of the laplace plane. Advances in the Astronautical Sciences. Volume 150, pp. 2427 – 2442, 2013.
[27] Krag, H., Lemmens, S., Flohrer, T., Klinkrad, H. Global trends in achieving successful end-of-life disposal in LEO and GEO. 13th International Conference on Space Operations, SpaceOps 2014, Pasadena, CA, United States, 5 – 9 May 2014, Code 105236.
[28] Fernandez, J.M., Visagie, L., Schenk, M., Stohlman, O.R., Aglietti, G.S., Lappas, V.J., Erb, S. Design and development of a gossamer sail system for deorbiting in low Earth orbit. Acta Astronautica. Volume 103, pp. 204 – 225, 2014.
[29] Trofimov, S., Ovchinnikov, M. Optimal low-thrust deorbiting of passively stabilized LEO satellites. Proceedings of the International Astronautical Congress, IAC. Volume 7, pp. 5224 – 5229, 2013.
[30] Muhammad, A.K., Okamoto, S., Lee, J.H., Comparisons of Proportional and Active-force Controls on Vibration of a Flexible Link Manipulator Using a Piezoelectric Actuator through Calculations and Experiments, IAENG, Engineering Letters, Volume 22, Issue 3, pp. 134 – 141, 2014.
[31] Tashakori, A., Ektesaabi, M., Position Sensors Fault Tolerant Control System in BLDC Motors, IAENG, Engineering Letters, Volume 21, Issue 1, pp. 39 – 46, 2014.
[32] Mahamood, M.R., Improving the Performance of Adaptive PDPID Control of Two-Link Flexible Robotic Manipulator with ILC, IAENG, Engineering Letters, Volume 20, Issue 3, pp. 259 – 270, 2012.
[33] Aslanov, V.S., Dynamics of free dual-spin spacecraft, IAENG, Engineering Letters, Volume 19, Issue 1, pp. 271 – 278, 2011.
[34] Kobayashi, T., Tsuba, S., Sliding Mode Control of Space Robot for Unknown Target Capturing, IAENG, Engineering Letters, Volume 19, Issue 2, 105 – 111, 2011.
[35] Tsuda, S., Sakano, K., Robust adaptive control of a large spacecraft, IAENG, Engineering Letters, Volume 16, Issue 3, pp. 321 – 325, 2008